In-situ methane enrichment in continuous anaerobic digestion of pig slurry by zero-valent iron nanoparticles addition under mesophilic and thermophilic conditions

Míriam Cerrillo,[a] Laura Burgos,[a] Beatriz Ruiz,[a] Raquel Barrena,[b] Javier Moral-Vico,[b] Xavier Font,[b] Antoni Sánchez[b] and August Bonmatí[a]*

[a] IRTA. GIRO. Torre Marimon. E-08140, Caldes de Montbui, Barcelona (Spain).
[b] GICOM, Department of Chemical, Biological and Environmental Engineering, Universitat Autònoma de Barcelona, Edifici Q, 08193 Cerdanyola del Vallès, Barcelona (Spain).
* Corresponding autor e-mail: august.bonmati@irta.cat

ABSTRACT

The effect of zero-valent iron nanoparticles (nZVI) addition on methane production during anaerobic digestion of pig slurry was assessed. Experiments were conducted using two experimental set-ups: batch and long-term continuous operation at a fixed nZVI dosage. Two different temperature operation ranges (mesophilic and thermophilic) were assessed. Biogas production and methane content were monitored, and the specific methanogenic activity of the biomass and nZVI oxidation state were evaluated at different times. The results of batch experiments at mesophilic temperature operation showed an inhibition of methane production at all tested dosages (42, 84, 168 and 254 mg_{nZVI} g^{-1} VSS concentrations), while methane production was boosted with the lowest dosage in thermophilic temperature operation. In continuous operation, nZVI addition produced an increase in methane content of biogas, achieving values between 80-85% in both temperature ranges. The average methane production rate increased 165% and 94% with respect to the control in thermophilic and mesophilic temperature range, respectively. The oxidation state of nZVI showed a value of +3 almost immediately after contact with substrate and a slower progressive oxidation during the reactors operation. The obtained results indicate that nZVI addition in anerobic digestion is an interesting straregy for in situ biogas upgrading.

Keywords

Anaerobic digestion, nanoparticles, methane, iron zero-valent, pig slurry, biogas upgrading.

1. Introduction

Biogas is a biofuel obtained from anaerobic digestion with multiple uses since it can be directly burnt for thermal energy production or power generation. Biogas is mainly composed of methane (50-70%) and CO_2 (30-50%), and can be upgraded to natural gas grade to be suitable for other uses such as transport fuel and injection in natural gas grid [1]. Various energy demanding physical and chemical methods are used nowadays for biogas upgrading, based on CO_2 and CH_4 separation from the biogas stream, such as scrubbing, pressure swing adsorption (PSA) or membrane separation [2]. Alternatively, other technologies under development are based on the conversion of CO_2 to CH_4, such as the electromethanogenesis process that can take place in bioelectrochemical system (BES) [3].

The enhancement of methane production in anaerobic digestion is subject of constant research, and several technologies and techniques can be applied, such as bioaugmentation or co-digestion [4]. The application of nanoparticles (NPs) is receiving increasing attention as an approach to increase methane production in anaerobic digestion. NPs have been reported to be useful for wastewater treatment applications [5]. NPs could act as electron donors or acceptors and cofactor of important enzymes in various bioprocesses, which will enhance their yields [6]. The effect of different metallic nanoparticles on biogas production in anaerobic digestion has been studied, such as silver NPs on sewage sludge anaerobic digestion [7]; iron oxide (Fe_2O_3) and titanium dioxide (TiO_2) NPs on cattle manure anaerobic digestion [8]; iron oxide (Fe_2O_3) NP on two-stage anaerobic digestion with waste sludge [9]; TiO_2 NPs, on anaerobic digestion of lignocellulosic substrate [10]; magnetite and iron zero-valent, on anaerobic digestion of sludge [11]; magnetite on chicken litter anaerobic digestion [12]; or iron zero-valent, on anaerobic granular sludge [13]. Some studies have reported an inhibitory effect of NPs, which will produce toxic effects over microorganisms, generally dosage and specific NPs dependant [14]. A previous study with nano zero-valent iron (nZVI) has reported

inhibition of methanogenesis due to its disruption of cell integrity [15]. On the contrary, no ecotoxicity has been detected in other studies [16], or an increase in methane production has been reported when iron NP were added [13,17,18]. Several comprehensive reviews report the impacts of different kinds of nanoparticles on anaerobic digestion processes [6,19,20].

The use of nZVI in anaerobic digestion has been proposed as a biogas upgrading method, since it may improve the proportion of methane to the detriment of CO_2 [2]. This technique could be applied with a low investment cost and a minimum process complexity since it will not consist of CO_2 removal or adsorption (i.e. zeolites) phases, but direct CO_2 conversion into methane. In addition to biogas methane enrichment, it has been reported that biogas production is also enhanced by nZVI addition [21]. The impact of different nZVI concentrations on microbial growth has been also assessed, reporting that different conditions of substrate composition, pH or temperature produced changes in organic matter removal efficiencies [22]. Although the increasing amount of published research on the impacts of NPs on anaerobic digestion, most of the nZVI studies focus on batch and short term assays, and waste activated sludge usage. Only a few studies use high strength wastewater such as livestock manure as a substrate [21,23–25]. Short term batch investigations have reported an enhancement in methane production [26–29], while some longer term investigations showed an increase of methane production in the early stages of experiments, which is followed by an inhibition phase [30]. A methane production increase depending on NP dosage was reported in other studies [31,32].

To the extent of our knowledge, this study is the first to examine the effects of nZVI dosage onto anaerobic digestion of pig slurry on long term and continuously fed assays, and to compare mesophilic and thermophilic operation temperature conditions.

Additionally, although the effect of iron nanoparticles on anaerobic digestion has been previously reported, most of the published literature does not include much information about the behaviour of iron. In this work, the morphological and microstructural study of nZVI is

presented. Furthermore, a novel study on the evolution of the oxidation state of this material when added to the anaerobic medium has been performed.

The aim of this study was to evaluate the impact of nZVI on methane production during anaerobic digestion of pig slurry, both under mesophilic and thermophilic temperature conditions, and in batch and continuous operation. Methanogenic activity tests have been applied to assess the change of microbial biomass after NP addition. Furthermore, Scanning Electron Microscope (SEM) and Electron energy-loss spectroscopy in a transmission electron microscope (TEM-EELS) have been used to monitor the morphology, microstructure and oxidation state of the NPs.

2. Materials and methods

2.1 Nanoparticles and feeding substrate

nZVI NPs were synthesised adding a sodium borohydride ($NaBH_4$, ≥98%, Sigma-Aldrich) aqueous solution to a ferrous chloride (III) ($FeCl_3$, ≥98%, Sigma-Aldrich) aqueous solution, using milli-Q grade water, based on the methodology described elsewhere [33]. Briefly, for batch assays, 200 mL of 3.72 M sodium borohydride was added dropwise to 200 mL of 0.93 M ferrous chloride while the solution was vigorously stirred under a N_2 stream at room temperature. The obtained nZVI was rinsed with milli-Q grade water and purged with nitrogen gas. The final concentration of nZVI in the stock solution was 0.47 M.

For continuous assays, to reduce the volume of stock solution added to the reactors in each pulse, the concentration of the nZVI solution was increased. A 0.93 M concentrated nZVI stock solution was prepared, mixing 75 mL of 7.45 M sodium borohydride and 75 mL of 1.86 M ferrous chloride with the same methodology described for batch nZVI solution.

The pig slurry used as feeding was collected at Puigllong farm (Gurb, Barcelona, Spain), sieved (500 µm) and frozen (-20 ºC) up to its use, to assure stable composition during all the experiment.

2.2 Batch assays at different nZVI dosage

Batch experiments (biochemical methane potential tests) were conducted to investigate the effect of different concentrations of nZVI on the production of methane in pig slurry anaerobic digestion. 120 mL serum bottles were used for this purpose, and each condition was prepared in triplicate. These serum bottles were filled with a 50 g solution composed of the inoculum (4 g_{VSS} L^{-1}), pig slurry as substrate (4 g_{COD} L^{-1}) and the different concentrations of NP (0, 42, 84, 168 and 254 mg_{NP} g^{-1} VSS). These doses were based on previous assays performed by the authors in semi-continuous AD tests of sewage sludge, which had proven to be effective for methane production increase [34]. The digested sludge from a mesophilic and a thermophilic lab-scale anaerobic digesters were used as inoculums to test both operational temperature ranges. A control in triplicate, without pig slurry substrate, was included in the setup. The bottles were sealed with rubber stoppers and capped with aluminium crimp caps. The headspace was purged with N_2 for 5 min in order to remove O_2 and assure anaerobic conditions. The bottles were incubated for 40 days at 37±2 ºC and 55±2 ºC for mesophilic and thermophilic temperature ranges, respectively. Methane production was monitored periodically by taking a gas sample (0.2 mL) from the headspace with a syringe and analysing the gas composition by gas chromatography.

Biogas was accumulated in the serum bottles headspace until the end of the assay. Pressure monitoring indicated that there was no high overpressure, so microorganisms were not affected, and it was not necessary to empty the headspace. The cumulative methane yield (V_{CH4}, mL) of each serum bottle was calculated using the N_2 concentration, which should be constant throughout the assay, to correct the molar fractions as follows (Equation 1):

$$V_{CH_4} = V_h \frac{X_{N_2}^0 \cdot X_{CH_4}}{1 - X_{CH_4} - X_{CO_2}} \quad (1)$$

Where V_h is the headspace volume (mL) of the serum bottle, X^o_{N2} is the molar fraction of nitrogen measured at the beginning of the assay, and X_{CH4} and X_{CO2} are the molar fractions of CH_4 and CO_2, respectively, present in biogas determined by gas chromatography.

Pressure build-up along the assay was calculated by the increase in the number of moles determined by gas chromatography and the ideal gas equation (Equation 2).

$$PV=nRT \quad (2)$$

where P is pressure (atm), V is the serum bottle headspace volume (L), n is the number of mole of gas determined by gas chromatography (N_2, CH_4 and CO_2), R is ideal gas constant (0.082 atm L mol^{-1} K^{-1}), and T is temperature (K).

2.3 Continuous experimental set-up

Three lab-scale continuous stirred tank reactors (CSTR) were used for the experiments. Two of them were operated in mesophilic temperature range (36 ºC), and the third one was operated at thermophilic temperature range (55 ºC). The anaerobic digesters (AD) consisted of a cylindrical glass reactor (25 cm diameter, volume of 5 L) fitted with a heat jacket with hot water circulating to keep the temperature at the desired value. A temperature probe was placed into the reactor lid for temperature monitoring. Continuous mixing was supplied to each reactor using an overhead stirrer. Biogas production was measured with a gas counter (µFlow, Bioprocess Control AB, Sweden). All the digesters were already in operation, fed with pig slurry for more than a year.

2.4 Reactors operation

The three ADs were fed in a continuous mode with raw pig slurry with a hydraulic retention time (HRT) of 10 days for the thermophilic AD and 20 days for the mesophilic ADs. The pig slurry was diluted with tap water to obtain the desired organic load. The main characteristics of the diluted pig slurry were as follows: total solids (TS), 29±4 g kg^{-1}; volatile

160 solids (VS), 19±3 g kg^{-1}; total chemical oxygen demand (TCOD), 36±5 g kg^{-1}; total Kjeldahl
161 nitrogen (TKN), 2.4±0.5 g kg^{-1}; ammonia nitrogen, 1.7±0.5 g kg^{-1}. The reactors were operated
162 during 265 days in 3 different phases (Table 1), with an organic loading rate (OLR) of 1.7±0.4
163 kg_{COD} m^{-3} day^{-1} and 4.1±1.1 kg_{COD} m^{-3} day^{-1} in mesophilic and thermophilic reactors,
164 respectively.

165 In Phase 1, one of the mesophilic ADs was used as control (MC), while a weekly nZVI
166 pulse of 84 mg g^{-1} SSV was injected in the second mesophilic reactor (M). In turn, the
167 thermophilic (T) reactor received a nZVI weekly pulse of 42 mg g^{-1} SSV. The dosages were
168 chosen according to the results obtained in the batch assays performed, as will be described
169 in Section 3.1. The addition of nZVI corresponding to a week was added in a unique pulse.
170 In order to compare the results of the thermophilic reactor with a control, a previous 63-day
171 period of the same reactor before starting nZVI addition was considered as Phase 0.

172 In Phase 2, a weekly pulse of nZVI was injected in the MC reactor, in the same
173 conditions as it was applied in the M reactor in Phase 1. In the case of the T and M reactors,
174 the dosages applied in Phase 2 were equal to those applied in Phase 1 but divided into 2
175 injections per week.

176 Finally, in Phase 3, NP addition was stopped in all reactors, to determine if NPs effects
177 on biogas production and its composition (richness of CH_4 and CO_2) were long lasting.

178 Each phase was maintained at least for 3 HRT to ensure a stable operation. For each
179 experimental condition, methane production rate (L_{CH4} kg_{VS}^{-1} d^{-1}) and chemical oxygen
180 demand (COD) removal efficiencies were used as control parameters, by taking weekly
181 samples. Biogas composition was analysed on weekdays, to better understand the effect of
182 nZVI addition on the anaerobic digestion process.

183 **Table 1.** Operation phases of the mesophilic control (CM), mesophilic (M) and thermophilic
184 reactors (T).

Phase	Period (d)	Frequency of nZVI injection (times/week)	nZVI concentration of the pulse (mg_{NP} g^{-1} SSV_{added})

		CM	M	T	CM	M	T
0	63	-	-	0	-	-	-
1	125	0	1	1	-	84	42
2	70	1	2	2	84	42	21
3	70	0	0	0	-	-	-

185
186

187 **2.5 Specific methanogenic activities**

188 To determine the changes in metabolic pathways when nZVI was applied, sludge
189 samples were collected from each reactor at the end of Phase 1 and 2, and also at the end of
190 Phase 0 in the thermophilic reactor, to perform specific methanogenic activity tests (SMA).
191 Tests were carried out using 120 mL serum bottles, following the methodology described
192 elsewhere [35]. A volatile fatty acid (VFA) mix (acetate/propionate/butyrate, 70/20/10),
193 acetate, and H_2 were used as substrates. The serum bottles were filled with a 50 mL solution
194 of the mesophilic or thermophilic sludge (1.5 g_{VSS} L^{-1}), substrate (5 g_{COD} L^{-1}),
195 macronutrients, micronutrients and bicarbonate (1g $_{NaHCO3}$ $g_{CODadded}^{-1}$). A control duplicate
196 without the medium was included in the set-up. The bottles were sealed with rubber stoppers
197 and capped with aluminium crimp caps. The headspace was purged for 5 min with N_2 in order
198 to assure anaerobic conditions. H_2 substrate addition was performed by injection of 60 mL of
199 high purity H_2 gas (≥ 99'999%) through the septum once the serum bottle was sealed and
200 purged. The bottles were incubated for 60 days at 37±2 ºC and 55±2 ºC for mesophilic and
201 thermophilic temperature ranges, respectively. Methane production was monitored
202 periodically by taking a gas sample (0.2 mL) from the head space with a gas-tight syringe and
203 analysing the gas composition by gas chromatography. Biogas was accumulated in the serum
204 bottles headspace until the end of the assay, and CH_4 volume and pressure build-up were
205 calculated as described in Equations 1 and 2.

206 The SMA was calculated from the linear increase in the CH_4 concentration at the
207 beginning of the experiments (when no lag phase was observed) divided by the amount of
208 VSS.

209

210 **2.6 Analytical methods and calculations**

211 Chemical oxygen demand (COD), ammonium nitrogen (NH_4^+-N), Kjeldahl nitrogen
212 (TKN), total and volatile solids (TS, VS), total suspended and volatile suspended solids (TSS,
213 VSS), pH, total and partial alkalinity were determined according to Standard Methods 5220
214 [36]. Partial alkalinity (PA), which corresponds roughly to bicarbonate alkalinity, was
215 determined by titration with H_2SO_4 from the original pH sample to pH 5.75. Total alkalinity
216 (titration to pH 4.3) corresponds to VFA alkalinity added to bicarbonate alkalinity [37]. The
217 bulk solution pH in each sample was measured using a CRISON 2000 pH electrode. N-NH_4^+
218 and TKN were analysed by a Büchi KjelFlex K-360 distiller, and a Metrohm 702
219 SM autotitrator. Volatile fatty acids (VFA) were quantified by gas chromatography using a
220 VARIAN CP-3800 (Varian, USA) chromatograph equipped with a flame ionisation detector
221 (FID). Methane content in biogas was determined using a VARIAN CP-3800 (Varian,
222 USA) gas chromatograph equipped with a Hayesep® Q packed column (matrix 80/100) and
223 a thermal conductivity detector (TCD). A sample of 200 µL, which was taken from the
224 headspace of serum bottles (batch and SMA tests) or reactors (continuous assays) through the
225 septum, was manually injected by means of a gas tight syringe (500 µL Hamilton
226 Sampleblock Syringe) at a temperature of 180 ºC. The carrier gas was helium, with a flux of
227 40 mL min^{-1}. The oven and detector temperatures were set at 90 and 180 ºC, respectively.
228 Iron concentration of the effluent and of the reactor content was determined in Phase 3 of
229 operation by inductively coupled plasma optical emission spectroscopy (ICP-OES) (Optima
230 4300DV, Perkin-Elmer).

231 Data were analysed using one-way analysis of variance (ANOVA). Whenever
232 significant differences of means were found, the Tukey test at the 5% significance level was
233 performed for separation of means. Statistical analysis was performed using the R software
234 package (R project for statistical computing, http://www.r-project.org).

235

236 **2.7 Nanoparticles characterization**

237 Samples from the content of the reactors M and T were taken during Phase 1, on day
238 112 to 115 of operation (M reactor) and 176 to 179 (T reactor), to characterise nZVI structure
239 and oxidation state after a pulse. Samples were also taken during Phase 3, in order to monitor
240 the evolution of nZVI once the pulses were stopped, on days 226, 239 and 253 of operation
241 (mesophilic reactors) and 290, 303 and 317 (thermophilic reactor).

242 The characterization of nZVI in terms of size, distribution and morphology was
243 performed using a scanning electron microscope (SEM), with a Quanta FEI 200 FEG-ESEM
244 instrument, equipped for analysis of Energy Dispersive X-ray (EDX). A FEI Tecnai G2 F20
245 HR(S)TEM equipped with a Gatan Image Filter (GIF) Quantum SE 963 @ 200kV to obtain
246 EELS spectra was also used to analyse the size, distribution and morphology of nZVI.
247 Besides, selected areas electron diffraction images (SAED) was used to study the
248 microstructure of the material with high resolution images. The utility for measuring the
249 energy spectrum electron loss (EELS) was used to obtain information about the oxidation
250 state of nZVI.

251 The EELS spectra defines a L_{32} ratio, which corresponds to a defined oxidation state
252 of iron according to Tan et al [38]. According to them, a value of 2.99 of this ratio corresponds
253 to zerovalent iron, while oxidation states of +2 and +3 correspond to 3.99 and 4.55 L_{32} values
254 respectively. Two different types of tests were performed for comparison: test number 1
255 consisted in studying nZVI evolution in a batch test using a 25 mL hermetically closed and
256 nitrogenized bottle. This test was performed with two combinations: test 1a) nZVI in an
257 aqueous suspension up to 14 days, and test 1b) nZVI added to anaerobic inoculum + pig slurry
258 (anaerobic medium) at the same concentration of continuous reactors up to 7 days. In test
259 number 2, nZVI samples were collected from continuous reactors operated up to three days:
260 test 2a) mesophilic reactors, and test 2b) thermophilic reactors.

3. Results and discussion

3.1 Methane production in batch assays at different nZVI dosage

Specific methane productions and initial slopes obtained in the batch assays under mesophilic and thermophilic conditions are presented in Figure 1. For both temperature ranges, maximum specific methane productions were obtained with no NP addition (267.6 and 235.0 L_{CH4} kg_{VS}^{-1} for mesophilic and thermophilic operation, respectively). Under mesophilic conditions, increasing nZVI concentration decreased methane production. Differently, under thermophilic conditions, the concentrations of 0 and 42 mg_{NP} g^{-1} VSS achieved similar methane production, with no significant statistical differences ($p < 0.05$). Interestingly, all NP concentrations boosted methane production during the first 20 days of the thermophilic batch assay, as it is shown by the initial slopes. Figure S1 shows the accumulated methane production of the different tested conditions. It is difficult to compare the obtained results with previous reports because of the different ways of expressing NP dosage. Most studies report the dosage in terms of volume (mg L^{-1}), when in other works it is preferred to express it as a function of the organic matter present in the substrate, as stated by Lizama and coworkers [39]. The nZVI concentrations tested in this assay were between 2.5 and 15.4 mM, and previous works have reported an inhibition of methanogenic activity with increasing concentrations of nZVI in mesophilic glucose anaerobic digestion (in a range of 1 to 30 mM) [15]. Other work has reported an increase in specific biogas and methane production in cattle manure batch mesophilic anaerobic digestion when increasing nZVI concentrations from 5 to 20 mg L^{-1} [21]. Batch assays with poultry litter and nZVI at 15, 50 and 100 mg L^{-1} (1.68, 5.58 and 11.17 mg_{NP} g^{-1} VS) increased methane production up to 29.1% compared to no nZVI addition [24]. Finally, adding 9 mg_{NP} g^{-1} VS to sewage sludge mesophilic anaerobic batch assays increased biogas yield and methane content 135% and

186%, respectively, with respect to control [39]. The concentrations of these assays are also lower than the ones tested in this assay, which range from 140 to 860 mg L^{-1}.

Wu and coworkers (2015) tested ZVI in batch anaerobic digestion of swine manure, although using powder form instead of NP, with concentrations as high as 50 g L^{-1}. It was reported that although methane production increased with the applied dose, excessive ZVI doses did not stimulate methane production further and probably exerted negative effects on microbial activity [40]. The addition of 5 g L^{-1} of ZVI powder to ammonia-rich swine manure batch anaerobic digestion was reported to achieve 54.2% higher methane yield relative to control [41].

This batch assay results show a clear inhibition of methane production in mesophilic temperature conditions and an initial methane boost in thermophilic conditions, which may be due to an excessive dosage compared to other works. Other possible inhibition causes in batch assays are discussed later in Section 3.2.4.

Regarding the different behaviour between mesophilic and thermophilic conditions, it has been reported previously and improvement in COD removal efficiency when increasing AD temperature from 37 ºC to 50 ºC with a 50 g L^{-1} addition of nZVI (13.37% and 33.43%, respectively), while the control reactor reduced its activity with the increase of temperature [22]. Furthermore, in this study, the thermophilic inoculum used in batch assays was obtained from the thermophilic reactor used in continuous operation mode. This reactor had been operated in previous assays with high organic and nitrogen loading rates, and hydrogenotrophic methanogens represented a high proportion of methanogenic archaea [42]. Biomass may be better acclimated and able to shift to hydrogenotrophic methanogenic metabolic pathway compared to the mesophilic temperature reactor, as the results of the SMA test have also shown (Section 3.3).

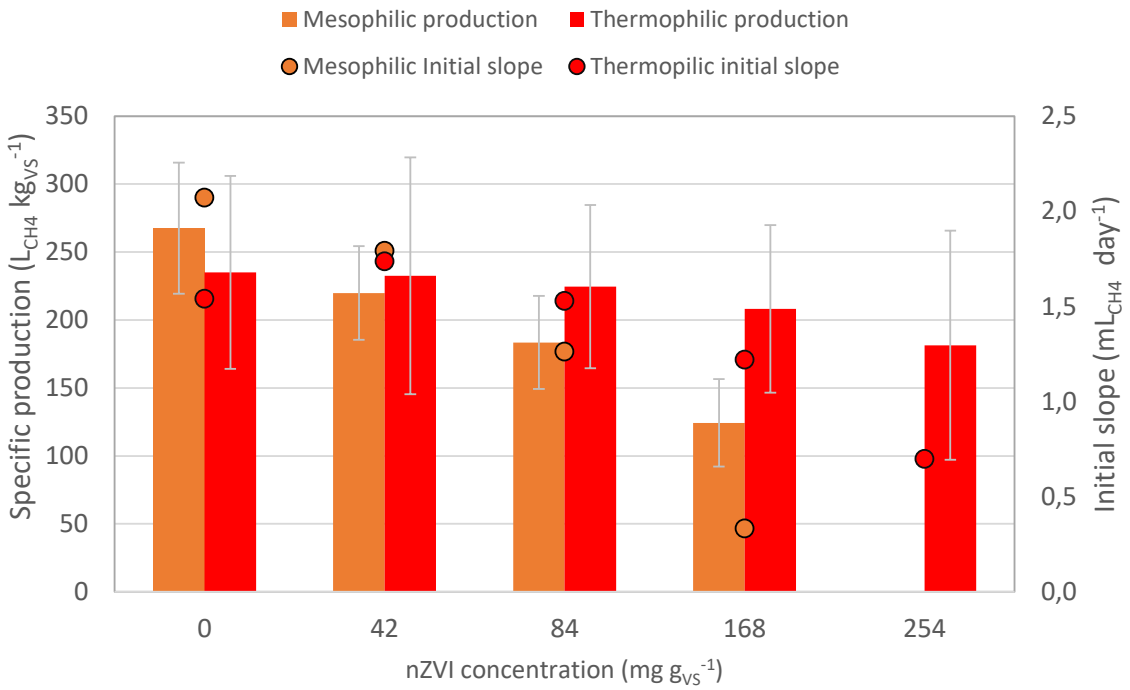

Figure 1. Specific methane production and initial slope of the batch assays performed in mesophilic and thermophilic temperature conditions with different nZVI dosages.

Although batch assays results have not shown a clear improvement in methane production, previous assays of the group in semi-continuous operation mode had proven to increase methane production in AD of sewage sludge in the tested dose range [34]. Consequently, the doses chosen to be tested in continuous operation assay were in the low concentration range, 84 and 42 mg_{NP} g^{-1} VSS_{added} for mesophilic (M) and thermophilic (T) reactors, respectively, to test if inhibition could be avoided in continuous operation mode, and to be able to compare the results obtained in both operation modes. Furthermore, continuous operation mode could have an acclimation effect on the biomass that may result in different behaviour of the anaerobic digestion process compared to batch tests [34].

3.2 Methane production in continuous assays with nZVI addition

3.2.1 Thermophilic temperature range operation

An increase in the content of methane in the biogas was produced with nZVI addition in continuous anaerobic digestion. As shown in Figure 2a, the percentage of methane in the thermophilic reactor increased from 64% in Phase 0 to a maximum value of 87% in Phase 1. Methane content showed an increase after each weekly pulse of nZVI, which was maintained for several days, followed by a decrease, until a new pulse was added. The boost in methane content was produced shortly after the nZVI pulse was added to the reactor (in the range of hours), as shown in the inset of Figure 2a. Previous work has reported that more than 90% of the total H_2 volume delivered by nZVI was produced in the first hour, regardless of initial nZVI concentration [43]. The same authors described that nZVI is easily deactivated during the dissolution process because of the formation of iron-related precipitates on its surface, due to its strong reducing power, resulting in much slower H_2 production rates after the first hour of dissolution.

a)

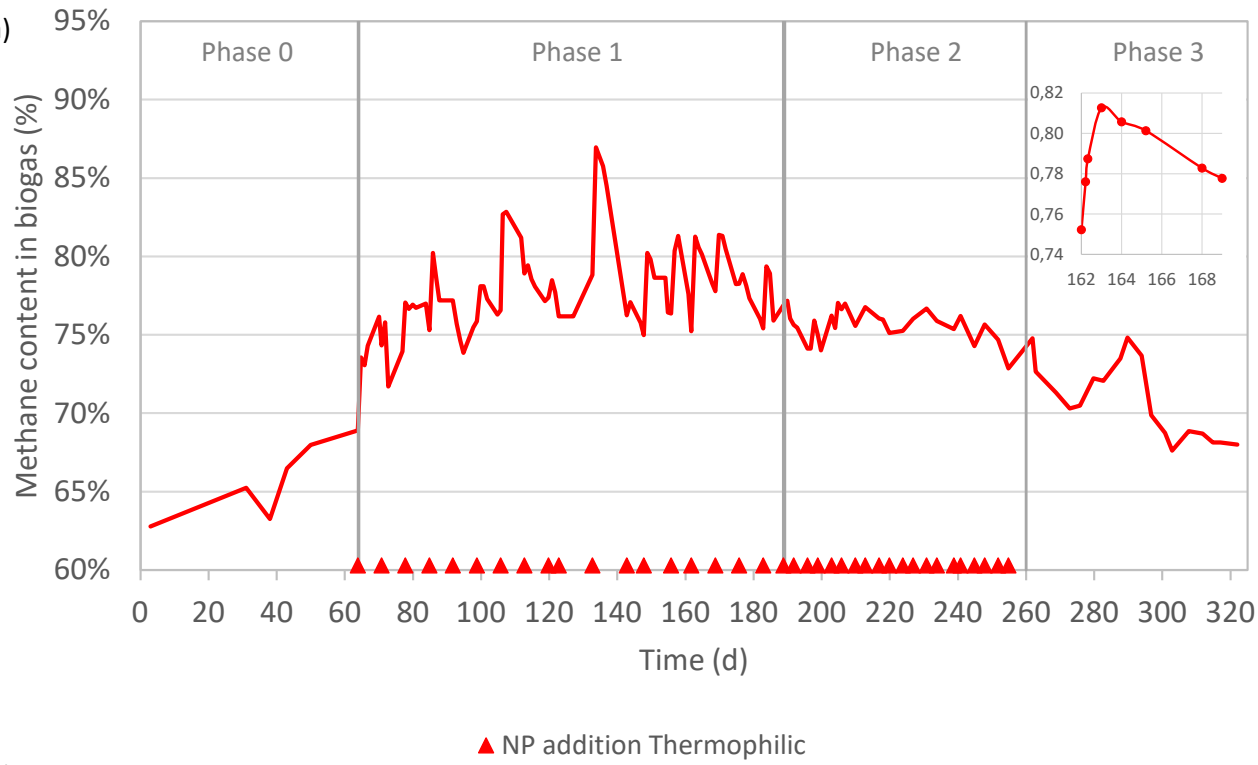

b)

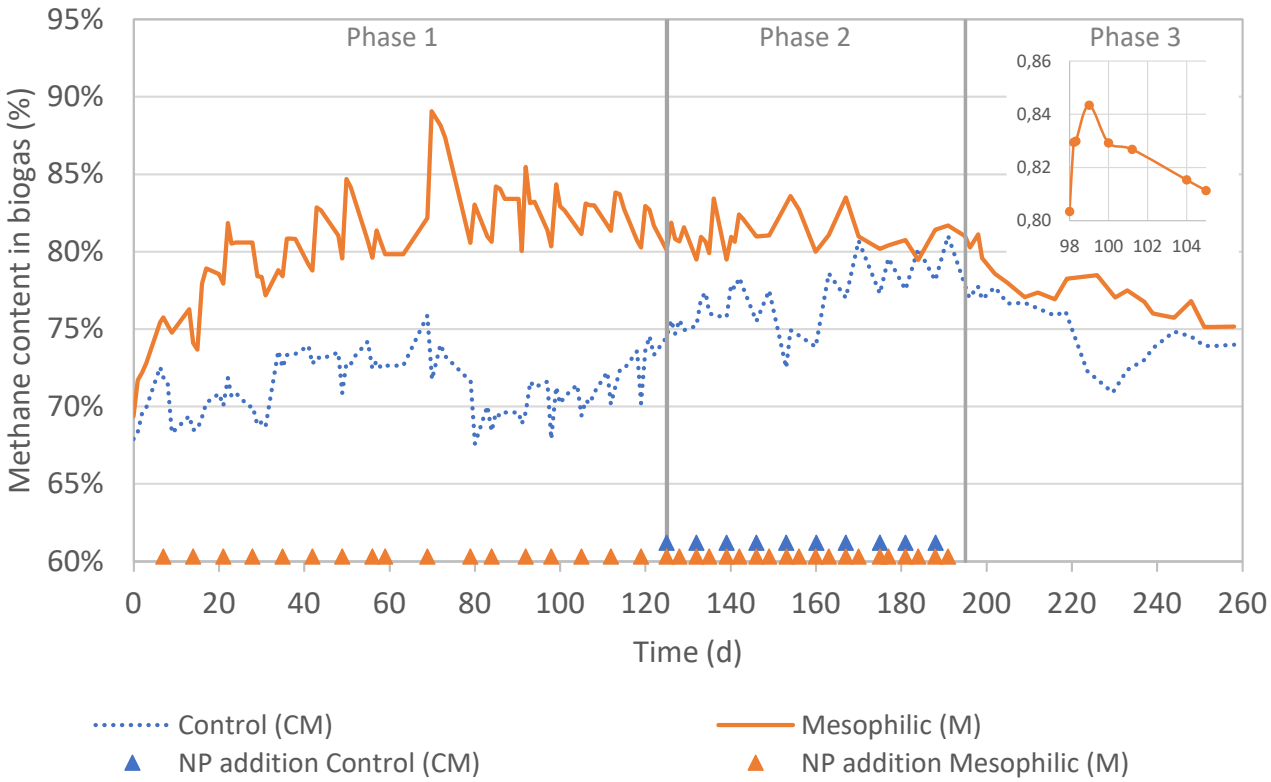

Figure 2. Methane content in biogas in the different phases of operation in a) thermophilic temperature conditions in reactor T (detail in the inset of the peak from day 162 to 169); b) mesophilic temperature conditions in reactors CM and M (detail in the inset of the peak of M reactor from day 98 to 105).

During Phase 2, when the weekly dosage was split into two pulses per week, the peaks were of less magnitude, but the average value was maintained (Table 2). With the nZVI pulses suppression, in Phase 3, the methane content in biogas showed a sustained decrease, returning to values that were similar to phase 0. This behaviour shows that the nZVI accumulated in the reactor in the previous phases has a delayed background effect on the operation. Previous studies have shown the long-lasting effect of nZVI, since depending on the degree of crystallinity of the particles, complete oxidation of Fe(0) could last between two weeks and a year [44,45]. Indeed, Fe concentration evaluation during Phase 3 (Figure S2) showed that 0.45 mg_{Fe} g^{-1} were still present in the effluent 10 days after the last nZVI pulse. The effluent and reactor content Fe concentration decreased to 0.05 mg_{Fe} g^{-1} 65 days after the last pulse, following the biogas methane content decreasing tendency during Phase 3. The fate of nZVI after being corroded to Fe^{2+} in the anaerobic digester is probably the formation of insoluble

siderite ($FeCO_3$), by interaction with CO_2; or the precipitation with PO_4^{3-} to form vivianite ($Fe_3(PO_4)_2$), as described in both cases by Puyol and co-workers (2018) [46].

Table 2. Main operational results of the three reactors, mesophilic control (MC), mesophilic (M) and thermophilic (T) in the different phases (mean±standard deviation).

Phase	Reactor	Methane content in biogas (%)	Methane production ($L\ kg_{VS}^{-1}\ d^{-1}$)	COD removal (%)	pH	Total Alkalinity ($g\ CaCO_3\ L^{-1}$)	Partial Alkalinity ($g\ CaCO_3\ L^{-1}$)
1	CM	71±2	214±78	50±9	8.1±0.2	7.2±0.8	6.5±0.9
2		77±2	404±100	46±11	8.2±0.1	10.7±1.4	9.4±1.3
3		75±2	342±88	49±11	8.3±0.1	11.1±1.0	9.8±0.7
1	M	81±4	255±85	48±10	8.3±0.1	7.6±1.2	6.7±1.0
2		81±1	402±128	45±12	8.5±0.3	10.3±1.2	8.8±1.1
3		78±2	321±118	52±15	8.4±0.1	10.8±0.7	9.9±0.6
0	T	66±2	65±22	31±10	8.2±0.1	9.2±0.9	7.6±0.8
1		78±3	140±57	40±10	8.2±0.2	6.4±0.7	5.6±0.6
2		76±1	172±56	45±13	8.4±0.1	9.7±1.0	7.7±1.0
3		71±2	146±54	50±9	8.2±0.1	9.1±1.2	7.7±0.9

The average methane production rate increased 165% during the nZVI application phases, from 65±22 to 172±56 $L_{methane}\ kg_{VS}^{-1}\ d^{-1}$ (Table 2, Figure S3). Finally, no significant statistical differences were found in the COD removal efficiency in any operational phase, which presented averages in a range between 31% and 50% (Table 2). Since no significant increase in COD removal efficiency was observed, the increase in methane production may be due to hydrogenotrophic methanogens H_2 (produced by nZVI corrosion) uptake and reaction with CO_2.

3.2.2 Mesophilic temperature range operation

Regarding the mesophilic reactors, a clear increase in methane content in biogas of M reactor compared to control (MC) was produced in Phase 1 (Figure 2b). Values of 88% were reached in M reactor, while methane content in MC was in a range of 67-69%. As in the thermophilic reactor, the increase of methane content was produced some hours after the pulse and was followed by a decrease at the end of the week.

When nZVI was added also to CM reactor (Phase 2), the methane content of biogas increased and reached the values obtained in the M reactor, over 80% during the peak. On the other hand, reactor M showed a more stable methane content value when the dosage was divided into two pulses a week (Figure 2b).

In Phase 3, methane content percentages started to decrease in both reactors in a steady way, as described for the thermophilic reactor. Fe concentration in mesophilic reactors during Phase 3 (Figure S2) showed higher values compared to T reactor, since the HRT was double than in T reactor. Fe concentration was the highest in M reactor, maybe due to differences in mixing efficiency compared to CM reactor. The effluent of M and CM reactors contained 1.5 and 0.9 $mg_{Fe}\ g^{-1}$, respectively, 10 days after the last pulse, which decreased to 0.48 and 0.18 $mg_{Fe}\ g^{-1}$ on day 65. Fe concentration in the effluent in Phase 3 correlates well with the slightly higher methane content of M reactor compared to CM reactor, and the faster decrease observed in T reactor.

The methane production rate average values in Table 2 show that reactor M produced 20% more methane during Phase 1 than reactor CM, with a total increase of 94% in Phase 2. The methane production of both reactors was similar in Phase 2, when CM reactor was submitted to nZVI addition, with a 94% improvement in the CM reactor (Figure S2). The COD removal efficiencies were similar in both reactors in all the phases, as shown in Table 2, similar to the behaviour described for the thermophilic reactor.

3.2.3 Other operation parameters evolution

Regarding other control parameters, data corresponding to pH, alkalinity and VFA is presented as Supporting Information. pH of the 3 reactors oscillated in general between 8.0 and 8.5 (Figure S4a and Figure S5a). Other authors have reported inhibition of the AD process at pH over 8.0 [47,48], but in this study, reactors performed in a stable way in all the operation time. An increase in pH has been reported due to the consumption of bicarbonate by

hydrogenotrophic methanogens [48]. Previous research articles have reported that pH may increase or remain stable with the addition of nZVI, according to Equations 3 and 4 [22,49].

$$4Fe_0 + 8H^+ + CO_2 \dashrightarrow 4Fe^{2+} + CH_4 + 2H_2O \quad (3)$$

$$Fe_0 + 2H_2O \dashrightarrow Fe^{2+} + H_2 + 2OH^- \quad (4)$$

In this study, no significant statistical differences have been observed comparing CM and M reactor pH or the different operation phases (Table 2). Regarding TA and PA, all reactors showed an increase in Phase 2 (Figure S4b and Figure S5b-c), that can be related to the increase in VFA of the influent in this phase (Figure S4c-d and Figure S6). This increase in the VFA content of the influent may also explain the temporal accumulation of acetic and propionic acid in this phase, rather than being produced by methanogens inhibition.

3.2.4 Influence of AD operation mode on nZVI effect

The observed improvement in methane production in continuous operation mode may be due to different nZVI effects. On the one hand, the release of hydrogen during nZVI corrosion/oxidation (Equation 3) can serve as the electron donor for methanogens [13,50], activating hydrogenotrophic metabolic pathway (Equation 5); and homoacetogens, for the production of acetic acid (Equation 6), which in turn could be converted into methane by acetoclastic methanogens (Equation 7) [51].

$$4H_2 + CO_2 \rightarrow CH_4 + 2H_2O \quad (5)$$

$$4H_2 + 2CO_2 \rightarrow CH_3COO^- + H^+ + 2H_2O \quad (6)$$

$$CH_3COO^- + H^+ \rightarrow CH_4 + CO_2 \quad (7)$$

On the other hand, nZVI may facilitate electron conduction. Several studies have shown that iron nanoparticles can accelerate direct interspecies electron transfer (DIET) [52]

between bacteria and methanogens [53]. Other relative larger conductive materials that have been tested in AD, such as biochar [54] or granular activated carbon [55,56] may be used by syntrophic microorganisms as an attaching surface. Differently, NPs attach to conductive pili, reducing the requirement of multi-heme *c*-type cytochromes for DIET [53].

The activity stimulation of key enzymes related to hydrolysis and acidogenesis has been reported in the AD of waste activated sludge (WAS) [57]. Hydrolysis of organic compounds to soluble substances is the rate-limiting step of AD when complex particulate organic matter predominates in the substrate.

Finally, nZVI may also react with toxic substances in the reactor, such as ammonia nitrogen [5,41] or hydrogen sulphide (H_2S) [24], lowering their concentration and alleviating inhibition phenomena on acetogens and methanogens.

The different behaviour of anaerobic digestion process observed in batch and continuous assays in this study may be due to an excess concentration of nZVI in relation to the total volume of the vial and reactors. The applied dosage was related to the amount of VSS that were added with the feeding. In the case of the continuous operation, each weekly pulse contributed to 0.6-0.7 g_{NP} L^{-1} with respect to the total volume of the reactor at the moment of application, which is in the range of the higher dose tested in batch assays. But, if this amount was distributed along the week, it would correspond to a concentration of 86-103 mg_{NP} L^{-1}. These values are in the range of the successful concentrations used in the studies referenced in the batch assays section.

Furthermore, in batch assays, the released H_2 by corrosion of nZVI could accumulate in the headspace due to rapid nZVI dilution and produce inhibition, accompanied by reductive decomposition of cell membrane [43]. Furthermore, the possible increase of pH described in Equation 3 or a possible accumulation of VFA due to the improvement of hydrolysis step [57] may have adversely impacted methanogenesis in batch operation, while fresh substrate addition may have helped to alleviate this effect in continuous operation [58].

3.3 Specific methanogenic activity

SMAs of the biomass of the three reactors were determined at the end of Phase 1 and Phase 2, besides Phase 0 in T reactor (Table 3, Figure S3). M reactor showed lower SMA values for all substrates than CM reactor, except for SMA_{H2} in phase 2. SMA values of CM reactor also decreased in Phase 2, when nZVI was added. Using the VFA mix as a substrate decreased the SMA in comparison to the acetic acid substrate in mesophilic temperature conditions in both reactors. This reduction may be due to an inhibition of propionate or butyrate degrading bacteria. No inhibition of the acetoclastic methanogenesis metabolic pathway has been detected, corroborating the fact that the accumulation of acetic acid during Phase 2 was not due to acetoclastic methanogens inhibition.

Table 3. Specific methanogenic activity (SMA) at the start of the assay (Phase 0), and end of Phase 1 and Phase 2 of the biomass of mesophilic control (MC), mesophilic (M) and thermophilic (T) fed with different substrates. ND: not determined.

Phase	Reactor	SMA (mg COD_{CH4} g_{VSS}^{-1} day^{-1})			
		VFA mix	Acetate	H_2	Blank
1	CM	198	281	22	1
2		156	210	16	1
1	M	111	239	11	2
2		71	209	22	4
0	T	189	ND	27	6
1		193	103	83	2
2		120	218	71	3

Regarding T reactor, it showed a higher SMA value with H_2 substrate than the one obtained for mesophilic reactors, which suggests better acclimatisation. The addition of nZVI boosted SMA with acetic acid and H_2 substrates, which produced a 2-times increase from Phase 1 to Phase 2 and a 3-times increase from Phase 0 to Phase 1, respectively. On the contrary, the VFA mix SMA was reduced 36% from Phase 0 to Phase 2. The activation of the hydrogenotrophic metabolic pathway correlates well with methanogens using hydrogen released during nZVI corrosion/oxidation as an electron donor.

Although the evolution of the SMA_{H2} in T reactor correlates well with the improvement shown in continuous operation, and the possibility that H_2 production by nZVI corrosion may enhance hydrogenotrophic metabolical pathway, the results obtained in M reactor compared to CM reactor are not so conclusive. As it has been shown by the results of the continuous assays, the effect of nZVI addition on methane production is especially remarkable a few hours after the pulse. Therefore, once the pulses were suppressed in Phase 3, the system returned slowly to the initial values. Furthermore, Fe oxidation may accelerate once the inoculum is exposed to air for assay preparation. Therefore, the effect of nZVI on biomass may have diluted during the SMA assays.

3.4 Morphologic and microstructural characterisation of nZVI

The SEM images obtained for the morphological characterization of nZVI showed the typical aggregation that occurs due to the existence of Van der Waals forces [59] (Figure 3a). The size of the observed particles, which describe spherical formations, were between 10 and 20 nm in diameter (Figure 3a). This aggregation was observed in TEM with a worm-like shape (Figure 3b). These formations for the nZVI observed with TEM are widely described in the literature [60]. It is clearly observed, as well, how once the oxidation process of NPs begins, a needle configuration on the outside is formed, configuring a rough morphology of these as observed in Figure 3c, which may be due to the formation of iron oxides and oxohydroxides [61]. These formations can also be seen in TEM images (Figure 3d, e), as mentioned in the next section on oxidation of Fe NPs. TEM images also showed the contact between nZVI and bacteria present in the reactors (Figure 3f).

A high resolution TEM image (Figure 3g) and an electron diffraction image of selected areas (SAED) (Figure 3h) revealed the existence of iron microcrystals with crystalline planes belonging to phases existing in the sample like the α phase of iron, and other iron oxides phases. It is very likely to have iron oxohydroxides of the FeOOH type, which cannot be

identified with this technique due to their amorphous nature. All the analysed images presented a typical interplanar distance of the α-Fe of about 0.21 nm [62]. Other typical interplane distances of some iron oxides such as 0.14 nm and 0.25 nm [61] can be observed as well, which indicates that a part of the analysed samples presents a certain degree of oxidation, and therefore the coexistence of oxidized and unoxidized Fe. This fact coincides with the hypotheses raised in the literature [62], which state that oxidized and unoxidized areas coexist, and oxidation occurs in the external parts of the nanoparticle, as confirmed in the next section of this work. The plane distances found in all the samples analysed are very similar, with very little variability among them.

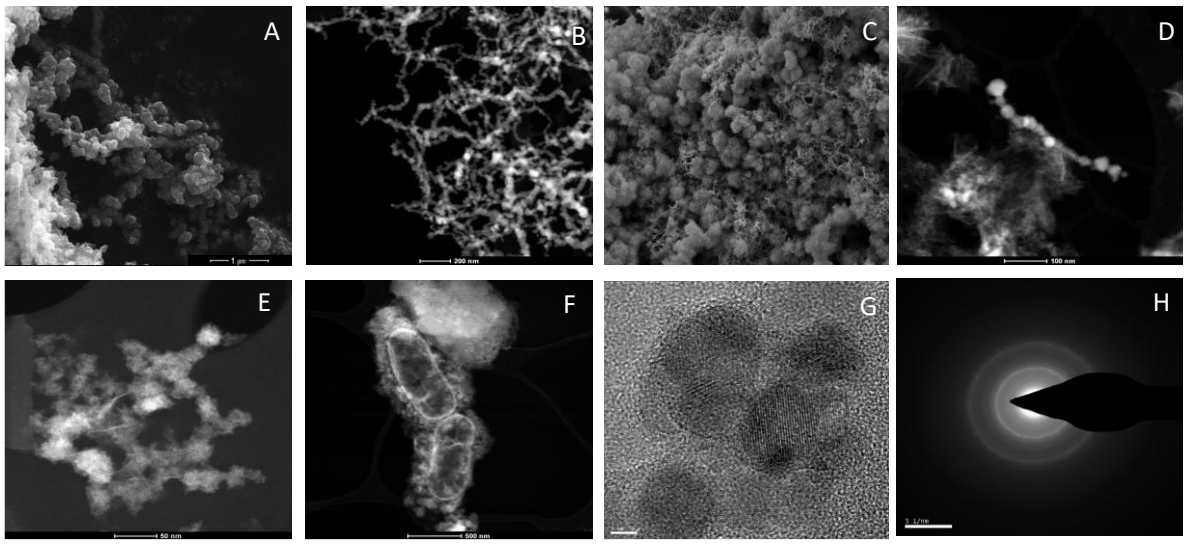

Figure 3. SEM images of: a) freshly synthesized nZVI, c) nZVI one day after synthesis; TEM images of: b) freshly synthesized nZVI, d) nZVI one day after synthesis, e) nZVI from a thermophilic reactor 10 min after addition, f) nZVI-bacteria contact in a nitrogenised bottle (test 2), in the 6th day after addition, g) high resolution image of freshly synthesized nZVI, h) SAED pattern of freshly synthesized nZVI.

3.5 Oxidation state evolution of nZVI

The evolution of the oxidation states of nZVI over the days based on the information on the L_{32} index can be seen in Table 4. The time scale observed in Table 4 starts when nZVI is added to the bottle containing water (test 1a), anaerobic medium (test 1b), or to the continuous reactors (tests 2a, b), and day 1 means that the sample is taken 24 hours later. As

seen, within the experimental variability, the oxidation state of nZVI in test 1a) is maintained up to 14 days at L_{32} values of around 4, which corresponds to a +2 oxidation state of iron. Right after synthesis, nZVI is a little oxidized, but L_{32} ratio (3.3) is near theoretical 2.99 corresponding to a zerovalent oxidation state. It can be stated that from the first day after the synthesis, particles increase their oxidation state to +2. However, the L_{32} ratio does not go beyond 4.2 after 14 days of the synthesis, which corresponds to an oxidation state between +2 and +3. This fact contrasts with the oxidation state evolution observed when nZVI is added to anaerobic medium both in tests 1b) and 2a, b), which entails an immediate oxidation to a +3 state, a level that was not reached even after 14 days when nZVI is in an aqueous suspension. In fact, only 10 minutes were necessary to reach that level of oxidation, which indicates that this process happens very quickly once nZVI comes into contact with anaerobic medium. The three tests (1b, 2a, 2b) performed including nZVI and anaerobic medium show very similar behaviour in terms of oxidation state evolution, with slightly faster oxidation for real reactors, even a little faster in the case of the thermophilic reactor, agreeing with the fact that higher temperatures normally accelerate reactions. Besides, L_{32} ratio indicates a +3 oxidation state is reached immediately, and it does not stop growing during the development of the test, which indicates that nZVI has oxidation capacity beyond +3, which agrees with the statement mentioned in section 3.2.1 about the long-lasting oxidation of nZVI.

Table 4. L_{32} ratio data used for the evaluation of the oxidation state of nZVI in several tests up to 14 days.

	Day							
Oxidation State Evaluation Test	**0 – 10 min***	**0 – 60 min**	**1**	**2**	**3**	**6**	**7**	**14**
1a) nZVI	3.3	-	4.0	3.7	4.0	3.4	4.2	4.0
1b) nZVI+Substrate	4.5	4.7	4.7	5.2	5.4	6.0	6.7	-
2a) Mesophilic Reactor	4.8	-	5.2	-	5.7	-	-	-
2b) Thermophilic Reactor	4.7	-	5.4	-	5.9	-	-	-

*EELS Spectra in test 1a was only evaluated 10 minutes after synthesis, time scale for tests 1b, 2a and 2b starts at the moment nZVI is added to anaerobic medium.

552 Regarding the effects of oxidation state on morphology, two differentiated areas can
553 be observed in all samples, one with spherical iron NPs (Figure 3a) that are normally linked
554 with worm-like shapes observed in TEM images, as already mentioned in the previous section
555 (Figure 3c), and another area of needle-shaped material, which usually corresponds to species
556 of iron oxides and oxohydroxides (e.g. $FeCO_3$, Fe_3O_4, Fe_2O_3, $Fe(OH)_3$ and FeOOH) [61],
557 which is confirmed by the fact that these latter areas are always more oxidized than the others
558 when analysing their L_{32} index. These two areas normally coexist, as observed in Figure 3d.
559 It is also observed that the areas of needles are more numerous as the test progresses and that
560 their degree of oxidation increases quite consistently throughout the days. Thus, needle shapes
561 are scarcely observed in samples of freshly synthesized NPs, but their presence increases as
562 the tests proceed. In addition, the images reveal that nZVI oxidation starts at the surface of
563 the nanoparticles, which causes their hairy appearance as the oxidation proceeds (Figure 3e).
564
565 **3.6 Evaluation of anaerobic digestion with nZVI addition**
566 Although previous works have shown an improvement of methane yield with the
567 addition of nZVI in batch AD of livestock manure, as described in section 3.1, to the authors'
568 knowledge no continuous long-term operation assays have been reported. Different substrates
569 have been used in previous studies in continuous operation. However, the specific
570 characteristics of each substrate, such as pH, TS/VS, alkalinity or ammonia content, may
571 change the effect of nZVI addition [22]. Furthermore, in those studies ZVI is used in different
572 formats, such as scrap or iron powder. As particle size decreases, the surface-to-volume ratio
573 increases, probably changing the properties of the material [63]
574 Previous studies in semi-continuous mode mesophilic AD of sewage sludge have
575 reported an increase in methane content in biogas from 65.1% to 75.9% when dosing of 0.81
576 g L^{-1} nZVI every seven days [34]. An increase from 60 to 75% was achieved by digestion of
577 palm oil mill effluent with 16 g L^{-1} ZVI powder addition under mesophilic conditions [58].

Compared to other in-situ biological upgrading techniques applied to livestock manure, such as H_2 external addition, the final methane content in biogas in this study is above the results reported in other works. For example, Luo and co-workers (2012) reported 65% methane content when digesting cattle manure with direct addition of H_2 to the reactor [48], while Luo and Angelidaki (2013) reported 75% methane content when co-digesting cattle manure and whey in thermophilic conditions with the same biogas upgrading technique [47].

3.7 Economic and environmental challenges for nZVI addition to AD

The results obtained in this study show an improvement of methane production in continuous long-term anaerobic digestion operation. The achieved biogas methane content is near the values required for methane injection in the natural gas net. In this sense, an adjustment of nZVI dosages is needed in order to determine if natural gas quality grade can be achieved, in order to avoid further upgrading steps. This partial CO_2 conversion in the biogas would decrease upgrading costs if methane content needed further increase. In a moment when great efforts are being made to upgrade biogas according to its methane content, this strategy supposes a clear decrease in the environmental and economic impact of these processes. Furthermore, by nZVI addition method, the total methane mass is increased, differently to other physical or chemical biogas upgrading technologies based on CO_2 removal. Furthermore, such as other biological technologies, the process is performed at mild operational conditions, at moderate temperature levels and atmospheric pressure, contributing to the sustainability of the technique [1].

However, up to now in-situ nZVI addition to AD is not competitive compared to established biogas upgrading techniques. nZVI production methods must ensure the efficiency of the obtained NPs and be able to produce them at a large scale while maintaining the reproducibility in size and chemical composition. The critical point for nZVI production is the cost of $NaBH_4$. It has been reported that the cost of nZVI production was of 0.95€ g^{-1},

where $NaBH_4$ reactant represented 85% of this cost [64]. In order to be applicable at a large scale, nZVI cost has to be decreased, i.e. by using extracts obtained from natural products, such as leaves from oak trees [64] or alternative methods such as precision milling [65]. Further process costs reduction could be achieved by using waste streams as Fe source. Iron nanoparticles have been successfully biosynthetized from water treatment sludge, so the use of commercial chemical precursors with analytical grades (e.g. $FeSO_4$, $FeNO_3$ and $FeCl_2$) could be avoided [18]. The evaluation of the purity of these nanoparticles should be addressed, besides their efficiency in AD application for methane enhancement.

Finally, nanoparticles use may present an environmental challenge that needs to be evaluated. Life cycle assessment (LCA) of the use of different metallic nanoparticles in anaerobic digestion of manure has been recently performed [66]. That study reported that anaerobic digestion supplemented with NP reduced greenhouse gas emissions, acidification, eutrophication, resource depletion, ozone layer depletion potential and human toxicity potential compared with no supplemented process.

4. Conclusions

Batch and continuous assays have been performed in order to evaluate nZVI addition to anaerobic digestion of pig slurry, both in mesophilic and thermophilic temperature ranges. Long term continuous assays have shown a clear enhancement in methane content in biogas, in addition to an increase in methane production rate, while results in batch assays were less conclusive probably due to a low acclimation of microorganisms. Methane content in biogas in continuous operation achieved 88% and 87% in mesophilic and thermophilic conditions, respectively. The average methane production rate increased 165% and 94% with respect to the control in thermophilic and mesophilic temperature range, with nZVI dosages of 42 mg g^{-1} SSV and 84 mg g^{-1} SSV, respectively. nZVI showed rapid oxidation when mixed with the substrate, although the oxidation process was maintained at least for one week. Compared to

conventional techniques for biogas upgrading, in situ nZVI addition would represent a decrease in investment and operation costs, although the reduction of nZVI production cost must be achieved. Furthermore, CO_2 would be converted in CH_4, instead of removed, increasing the final methane production.

Conflicts of interest

There are no conflicts to declare.

Acknowledgements

This research was funded by the Spanish Ministry of Economy and Competitiveness (INIA project RTA2015-00079-C02-01). The support of the CERCA Program and of the Consolidated Research Group TERRA (ref. 2017 SGR 1290), both from the Generalitat de Catalunya, is also acknowledged.

References

[1] I. Angelidaki, L. Treu, P. Tsapekos, G. Luo, S. Campanaro, H. Wenzel, P.G. Kougias, Biogas upgrading and utilization: Current status and perspectives, Biotechnol. Adv. 36 (2018) 452–466. https://doi.org/https://doi.org/10.1016/j.biotechadv.2018.01.011.

[2] D. Dong, P. Aleta, X. Zhao, O.K. Choi, S. Kim, J.W. Lee, Effects of nanoscale zero valent iron (nZVI) concentration on the biochemical conversion of gaseous carbon dioxide (CO2) into methane (CH4), Bioresour. Technol. 275 (2019) 314–320. https://doi.org/https://doi.org/10.1016/j.biortech.2018.12.075.

[3] M. Cerrillo, M. Vinas, A. Bonmatí, Startup of electromethanogenic microbial electrolysis cells with two different biomass inocula for biogas upgrading, ACS Sustain. Chem. Eng. 5 (2017) 8852–8859. https://doi.org/10.1021/acssuschemeng.7b01636.

[4] M. Tabatabaei, M. Aghbashlo, E. Valijanian, H. Kazemi Shariat Panahi, A.-S. Nizami, H. Ghanavati, A. Sulaiman, S. Mirmohamadsadeghi, K. Karimi, A comprehensive review on recent biological innovations to improve biogas production, Part 2: Mainstream and downstream strategies, Renew. Energy. 146 (2020) 1392–1407. https://doi.org/https://doi.org/10.1016/j.renene.2019.07.047.

[5] T.W.M. Amen, O. Eljamal, A.M.E. Khalil, N. Matsunaga, Wastewater degradation by iron/copper nanoparticles and the microorganism growth rate, J. Environ. Sci. 74 (2018) 19–31. https://doi.org/https://doi.org/10.1016/j.jes.2018.01.028.

[6] M. Dehhaghi, M. Tabatabaei, M. Aghbashlo, H. Kazemi Shariat Panahi, A.-S. Nizami, A state-of-the-art review on the application of nanomaterials for enhancing biogas production, J. Environ. Manage. 251 (2019) 109597. https://doi.org/https://doi.org/10.1016/j.jenvman.2019.109597.

[7] A. Grosser, A. Grobelak, A. Rorat, P. Courtois, F. Vandenbulcke, S. Lemière, R. Guyoneaud, E. Attard, P. Celary, Effects of silver nanoparticles on performance of anaerobic digestion of sewage sludge and associated microbial communities, Renew. Energy. 171 (2021) 1014–1025. https://doi.org/https://doi.org/10.1016/j.renene.2021.02.127.

[8] M. Farghali, F.J. Andriamanohiarisoamanana, M.M. Ahmed, S. Kotb, T. Yamashiro, M. Iwasaki, K. Umetsu, Impacts of iron oxide and titanium dioxide nanoparticles on biogas production: Hydrogen sulfide mitigation, process stability, and prospective challenges, J. Environ. Manage. 240 (2019) 160–167. https://doi.org/10.1016/j.jenvman.2019.03.089.

[9] Z. Zhang, L. Guo, Y. Wang, Y. Zhao, Z. She, M. Gao, Y. Guo, Application of iron oxide (Fe3O4) nanoparticles during the two-stage anaerobic digestion with waste sludge: Impact on the biogas production and the substrate metabolism, Renew. Energy. 146 (2020) 2724–2735. https://doi.org/https://doi.org/10.1016/j.renene.2019.08.078.

683 [10] P. Ghofrani-Isfahani, H. Baniamerian, P. Tsapekos, M. Alvarado-Morales, T. Kasama,
684 M. Shahrokhi, M. Vossoughi, I. Angelidaki, Effect of metal oxide based TiO_2
685 nanoparticles on anaerobic digestion process of lignocellulosic substrate, Energy. 191
686 (2020) 116580. https://doi.org/https://doi.org/10.1016/j.energy.2019.116580.
687 [11] F. Suanon, Q. Sun, D. Mama, J. Li, B. Dimon, C.P. Yu, Effect of nanoscale zero-valent
688 iron and magnetite (Fe_3O_4) on the fate of metals during anaerobic digestion of sludge,
689 Water Res. 88 (2016) 897–903. https://doi.org/10.1016/j.watres.2015.11.014.
690 [12] G.S. Aguilar-Moreno, E. Navarro-Cerón, A. Velázquez-Hernández, G. Hernández-
691 Eugenio, M.Á. Aguilar-Méndez, T. Espinosa-Solares, Enhancing methane yield of
692 chicken litter in anaerobic digestion using magnetite nanoparticles, Renew. Energy.
693 147 (2020) 204–213. https://doi.org/https://doi.org/10.1016/j.renene.2019.08.111.
694 [13] C.-S. He, P.-P. He, H.-Y. Yang, L.-L. Li, Y. Lin, Y. Mu, H.-Q. Yu, Impact of zero-
695 valent iron nanoparticles on the activity of anaerobic granular sludge: From
696 macroscopic to microcosmic investigation, Water Res. 127 (2017) 32–40.
697 https://doi.org/https://doi.org/10.1016/j.watres.2017.09.061.
698 [14] H. Mu, Y. Chen, Long-term effect of ZnO nanoparticles on waste activated sludge
699 anaerobic digestion, Water Res. 45 (2011) 5612–5620.
700 https://doi.org/https://doi.org/10.1016/j.watres.2011.08.022.
701 [15] Y. Yang, J. Guo, Z. Hu, Impact of nano zero valent iron (NZVI) on methanogenic
702 activity and population dynamics in anaerobic digestion, Water Res. 47 (2013) 6790–
703 6800. https://doi.org/https://doi.org/10.1016/j.watres.2013.09.012.
704 [16] J. Gonzalez-Estrella, R. Sierra-Alvarez, J.A. Field, Toxicity assessment of inorganic
705 nanoparticles to acetoclastic and hydrogenotrophic methanogenic activity in anaerobic
706 granular sludge, J. Hazard. Mater. 260 (2013) 278–285.
707 https://doi.org/https://doi.org/10.1016/j.jhazmat.2013.05.029.
708 [17] R. Barrena, E. Casals, J. Colón, X. Font, A. Sánchez, V. Puntes, Evaluation of the

709 ecotoxicity of model nanoparticles, Chemosphere. 75 (2009) 850–857.
710 https://doi.org/https://doi.org/10.1016/j.chemosphere.2009.01.078.
711 [18] M. Yazdani, M. Ebrahimi-Nik, A. Heidari, M.H. Abbaspour-Fard, Improvement of
712 biogas production from slaughterhouse wastewater using biosynthesized iron
713 nanoparticles from water treatment sludge, Renew. Energy. 135 (2019) 496–501.
714 https://doi.org/https://doi.org/10.1016/j.renene.2018.12.019.
715 [19] B. Demirel, The impacts of engineered nanomaterials (ENMs) on anaerobic digestion
716 processes, Process Biochem. 51 (2016) 308–313.
717 https://doi.org/https://doi.org/10.1016/j.procbio.2015.12.007.
718 [20] Y.-J. Lee, D.-J. Lee, Impact of adding metal nanoparticles on anaerobic digestion
719 performance – A review, Bioresour. Technol. 292 (2019) 121926.
720 https://doi.org/https://doi.org/10.1016/j.biortech.2019.121926.
721 [21] E. Abdelsalam, M. Samer, Y.A. Attia, M.A. Abdel-Hadi, H.E. Hassan, Y. Badr,
722 Influence of zero valent iron nanoparticles and magnetic iron oxide nanoparticles on
723 biogas and methane production from anaerobic digestion of manure, Energy. 120
724 (2017) 842–853. https://doi.org/https://doi.org/10.1016/j.energy.2016.11.137.
725 [22] K. Bensaida, R. Eljamal, kareman Eljamal, Y. Sughihara, O. Eljamal, The impact of
726 iron bimetallic nanoparticles on bulk microbial growth in wastewater, J. Water Process
727 Eng. 40 (2021) 101825. https://doi.org/https://doi.org/10.1016/j.jwpe.2020.101825.
728 [23] E. Abdelsalam, M. Samer, Y.A. Attia, M.A. Abdel-Hadi, H.E. Hassan, Y. Badr,
729 Comparison of nanoparticles effects on biogas and methane production from anaerobic
730 digestion of cattle dung slurry, Renew. Energy. 87 (2016) 592–598.
731 https://doi.org/https://doi.org/10.1016/j.renene.2015.10.053.
732 [24] A. Hassanein, S. Lansing, R. Tikekar, Impact of metal nanoparticles on biogas
733 production from poultry litter, Bioresour. Technol. 275 (2019) 200–206.
734 https://doi.org/https://doi.org/10.1016/j.biortech.2018.12.048.

735 [25] W. Huang, F. Yang, W. Huang, Z. Lei, Z. Zhang, Enhancing hydrogenotrophic
736 activities by zero-valent iron addition as an effective method to improve sulfadiazine
737 removal during anaerobic digestion of swine manure, Bioresour. Technol. 294 (2019)
738 122178. https://doi.org/https://doi.org/10.1016/j.biortech.2019.122178.
739 [26] T.W.M. Amen, O. Eljamal, A.M.E. Khalil, Y. Sugihara, N. Matsunaga, Methane yield
740 enhancement by the addition of new novel of iron and copper-iron bimetallic
741 nanoparticles, Chem. Eng. Process. - Process Intensif. 130 (2018) 253–261.
742 https://doi.org/https://doi.org/10.1016/j.cep.2018.06.020.
743 [27] T. Jia, Z. Wang, H. Shan, Y. Liu, L. Gong, Effect of nanoscale zero-valent iron on
744 sludge anaerobic digestion, Resour. Conserv. Recycl. 127 (2017) 190–195.
745 https://doi.org/https://doi.org/10.1016/j.resconrec.2017.09.007.
746 [28] F. Suanon, Q. Sun, M. Li, X. Cai, Y. Zhang, Y. Yan, C.-P. Yu, Application of nanoscale
747 zero valent iron and iron powder during sludge anaerobic digestion: Impact on methane
748 yield and pharmaceutical and personal care products degradation, J. Hazard. Mater.
749 321 (2017) 47–53. https://doi.org/https://doi.org/10.1016/j.jhazmat.2016.08.076.
750 [29] J. Zhou, X. You, B. Niu, X. Yang, L. Gong, Y. Zhou, J. Wang, H. Zhang, Enhancement
751 of methanogenic activity in anaerobic digestion of high solids sludge by nano zero-
752 valent iron, Sci. Total Environ. 703 (2020) 135532.
753 https://doi.org/https://doi.org/10.1016/j.scitotenv.2019.135532.
754 [30] E. Kökdemir Ünşar, N.A. Perendeci, What kind of effects do Fe_2O_3 and Al_2O_3
755 nanoparticles have on anaerobic digestion, inhibition or enhancement?, Chemosphere.
756 211 (2018) 726–735.
757 https://doi.org/https://doi.org/10.1016/j.chemosphere.2018.08.014.
758 [31] Y. Zhang, Z. Yang, R. Xu, Y. Xiang, M. Jia, J. Hu, Y. Zheng, W. Xiong, J. Cao,
759 Enhanced mesophilic anaerobic digestion of waste sludge with the iron nanoparticles
760 addition and kinetic analysis, Sci. Total Environ. 683 (2019) 124–133.

761 https://doi.org/https://doi.org/10.1016/j.scitotenv.2019.05.214.
762 [32] Y. Zhang, Z. Yang, Y. Xiang, R. Xu, Y. Zheng, Y. Lu, M. Jia, S. Sun, J. Cao, W.
763 Xiong, Evolutions of antibiotic resistance genes (ARGs), class 1 integron-integrase
764 (intI1) and potential hosts of ARGs during sludge anaerobic digestion with the iron
765 nanoparticles addition, Sci. Total Environ. 724 (2020) 138248.
766 https://doi.org/https://doi.org/10.1016/j.scitotenv.2020.138248.
767 [33] S. Choe, S.-H. Lee, Y.-Y. Chang, K.-Y. Hwang, J. Khim, Rapid reductive destruction
768 of hazardous organic compounds by nanoscale Fe_0, Chemosphere. 42 (2001) 367–372.
769 https://doi.org/https://doi.org/10.1016/S0045-6535(00)00147-8.
770 [34] R. Barrena, M. del C. Vargas-García, G. Capell, M. Barańska, V. Puntes, J. Moral-
771 Vico, A. Sánchez, X. Font, Sustained effect of zero-valent iron nanoparticles under
772 semi-continuous anaerobic digestion of sewage sludge: Evolution of nanoparticles and
773 microbial community dynamics, Sci. Total Environ. 777 (2021) 145969.
774 https://doi.org/https://doi.org/10.1016/j.scitotenv.2021.145969.
775 [35] M. Cerrillo, L. Morey, M. Viñas, A. Bonmatí, Assessment of active methanogenic
776 archaea in a methanol-fed upflow anaerobic sludge blanket reactor., Appl. Microbiol.
777 Biotechnol. 100 (2016) 10137–10146. https://doi.org/10.1007/s00253-016-7862-4.
778 [36] APHA, Standard Methods for the Examination of Water and Wastewater, 20th ed.,
779 American Public Health Association, American Water Works Association, and Water
780 Pollution Control Federation, Washington, D.C., 1999.
781 [37] G.K. Anderson, G. Yang, Determination of bicarbonate and total volatile acid
782 concentration in anaerobic digesters using a simple titration, Water Environ. Res. 64
783 (1992) 53–59. https://doi.org/https://doi.org/10.2175/WER.64.1.8.
784 [38] H. Tan, J. Verbeeck, A. Abakumov, G. Van Tendeloo, Oxidation state and chemical
785 shift investigation in transition metal oxides by EELS, Ultramicroscopy. 116 (2012)
786 24–33. https://doi.org/https://doi.org/10.1016/j.ultramic.2012.03.002.

[39] A.C. Lizama, C.C. Figueiras, A.Z. Pedreguera, J.E. Ruiz Espinoza, Enhancing the performance and stability of the anaerobic digestion of sewage sludge by zero valent iron nanoparticles dosage, Bioresour. Technol. 275 (2019) 352–359. https://doi.org/https://doi.org/10.1016/j.biortech.2018.12.086.

[40] D. Wu, S. Zheng, A. Ding, G. Sun, M. Yang, Performance of a zero valent iron-based anaerobic system in swine wastewater treatment, J. Hazard. Mater. 286 (2015) 1–6. https://doi.org/https://doi.org/10.1016/j.jhazmat.2014.12.029.

[41] Y. Yang, F. Yang, W. Huang, W. Huang, F. Li, Z. Lei, Z. Zhang, Enhanced anaerobic digestion of ammonia-rich swine manure by zero-valent iron: With special focus on the enhancement effect on hydrogenotrophic methanogenesis activity, Bioresour. Technol. 270 (2018) 172–179. https://doi.org/https://doi.org/10.1016/j.biortech.2018.09.008.

[42] M. Cerrillo, M. Viñas, A. Bonmatí, Unravelling the active microbial community in a thermophilic anaerobic digester-microbial electrolysis cell coupled system under different conditions, Water Res. 110 (2017) 192–201. https://doi.org/https://doi.org/10.1016/j.watres.2016.12.019.

[43] Y.-X. Huang, J. Guo, C. Zhang, Z. Hu, Hydrogen production from the dissolution of nano zero valent iron and its effect on anaerobic digestion, Water Res. 88 (2016) 475–480. https://doi.org/https://doi.org/10.1016/j.watres.2015.10.028.

[44] Y. Liu, H. Choi, D. Dionysiou, G. V Lowry, Trichloroethene Hydrodechlorination in Water by Highly Disordered Monometallic Nanoiron, Chem. Mater. 17 (2005) 5315–5322. https://doi.org/10.1021/cm0511217.

[45] Y. Liu, G. V. Lowry, Effect of particle age (Fe_0 content) and solution pH on NZVI reactivity: H2 evolution and TCE dechlorination, Environ. Sci. Technol. 40 (2006) 6085–6090. https://doi.org/10.1021/es060685o.

[46] D. Puyol, X. Flores-Alsina, Y. Segura, R. Molina, B. Padrino, J.L.G. Fierro, K. V

Gernaey, J.A. Melero, F. Martinez, Exploring the effects of ZVI addition on resource recovery in the anaerobic digestion process, Chem. Eng. J. 335 (2018) 703–711. https://doi.org/https://doi.org/10.1016/j.cej.2017.11.029.

[47] G. Luo, I. Angelidaki, Co-digestion of manure and whey for in situ biogas upgrading by the addition of H2: process performance and microbial insights, Appl. Microbiol. Biotechnol. 97 (2013) 1373–1381. https://doi.org/10.1007/s00253-012-4547-5.

[48] G. Luo, S. Johansson, K. Boe, L. Xie, Q. Zhou, I. Angelidaki, Simultaneous hydrogen utilization and in situ biogas upgrading in an anaerobic reactor., Biotechnol. Bioeng. 109 (2012) 1088–1094. https://doi.org/10.1002/bit.24360.

[49] L. Liang, N. Korte, B. Gu, R. Puls, C. Reeter, Geochemical and microbial reactions affecting the long-term performance of in situ 'iron barriers,' Adv. Environ. Res. 4 (2000) 273–286. https://doi.org/https://doi.org/10.1016/S1093-0191(00)00026-5.

[50] K.-F. Chen, S. Li, W. Zhang, Renewable hydrogen generation by bimetallic zero valent iron nanoparticles, Chem. Eng. J. 170 (2011) 562–567. https://doi.org/https://doi.org/10.1016/j.cej.2010.12.019.

[51] I. Vyrides, M. Andronikou, A. Kyprianou, A. Modic, A. Filippeti, C. Yiakoumis, C.G. Samanides, CO_2 conversion to CH_4 using Zero Valent Iron (ZVI) and anaerobic granular sludge: Optimum batch conditions and microbial pathways, J. CO2 Util. 27 (2018) 415–422. https://doi.org/https://doi.org/10.1016/j.jcou.2018.08.023.

[52] A.-E. Rotaru, P.M. Shrestha, F. Liu, M. Shrestha, D. Shrestha, M. Embree, K. Zengler, C. Wardman, K.P. Nevin, D.R. Lovley, A new model for electron flow during anaerobic digestion: direct interspecies electron transfer to *Methanosaeta* for the reduction of carbon dioxide to methane, Energy Environ. Sci. 7 (2014) 408–415. https://doi.org/10.1039/C3EE42189A.

[53] S. Barua, B.R. Dhar, Advances towards understanding and engineering direct interspecies electron transfer in anaerobic digestion, Bioresour. Technol. 244 (2017)

698–707. https://doi.org/https://doi.org/10.1016/j.biortech.2017.08.023.

[54] Z. Zhao, Y. Zhang, T.L. Woodard, K.P. Nevin, D.R. Lovley, Enhancing syntrophic metabolism in up-flow anaerobic sludge blanket reactors with conductive carbon materials, Bioresour. Technol. 191 (2015) 140–145. https://doi.org/https://doi.org/10.1016/j.biortech.2015.05.007.

[55] Y. Dang, D.E. Holmes, Z. Zhao, T.L. Woodard, Y. Zhang, D. Sun, L.-Y. Wang, K.P. Nevin, D.R. Lovley, Enhancing anaerobic digestion of complex organic waste with carbon-based conductive materials, Bioresour. Technol. 220 (2016) 516–522. https://doi.org/https://doi.org/10.1016/j.biortech.2016.08.114.

[56] F. Liu, A.-E. Rotaru, P.M. Shrestha, N.S. Malvankar, K.P. Nevin, D.R. Lovley, Promoting direct interspecies electron transfer with activated carbon, Energy Environ. Sci. 5 (2012) 8982–8989. https://doi.org/10.1039/C2EE22459C.

[57] J. Luo, L. Feng, Y. Chen, X. Li, H. Chen, N. Xiao, D. Wang, Stimulating short-chain fatty acids production from waste activated sludge by nano zero-valent iron, J. Biotechnol. 187 (2014) 98–105. https://doi.org/https://doi.org/10.1016/j.jbiotec.2014.07.444.

[58] V. Domrongpokkaphan, C. Phalakornkule, M. Khemkhao, In-situ methane enrichment of biogas from anaerobic digestion of palm oil mill effluent by addition of zero valent iron (ZVI), Int. J. Hydrogen Energy. (2021). https://doi.org/https://doi.org/10.1016/j.ijhydene.2021.03.083.

[59] F. He, D. Zhao, Hydrodechlorination of trichloroethene using stabilized Fe-Pd nanoparticles: Reaction mechanism and effects of stabilizers, catalysts and reaction conditions, Appl. Catal. B Environ. 84 (2008) 533–540. https://doi.org/https://doi.org/10.1016/j.apcatb.2008.05.008.

[60] F.S. dos Santos, F.R. Lago, L. Yokoyama, F.V. Fonseca, Synthesis and characterization of zero-valent iron nanoparticles supported on SBA-15, J. Mater. Res.

Technol. 6 (2017) 178–183. https://doi.org/https://doi.org/10.1016/j.jmrt.2016.11.004.

[61] G. Zhen, X. Lu, Y.-Y. Li, Y. Liu, Y. Zhao, Influence of zero valent scrap iron (ZVSI) supply on methane production from waste activated sludge, Chem. Eng. J. 263 (2015) 461–470. https://doi.org/https://doi.org/10.1016/j.cej.2014.11.003.

[62] A. Liu, W. Zhang, Fine structural features of nanoscale zero-valent iron characterized by spherical aberration corrected scanning transmission electron microscopy (Cs-STEM), Analyst. 139 (2014) 4512–4518. https://doi.org/10.1039/C4AN00679H.

[63] H. Baniamerian, P.G. Isfahani, P. Tsapekos, M. Alvarado-Morales, M. Shahrokhi, M. Vossoughi, I. Angelidaki, Application of nano-structured materials in anaerobic digestion: Current status and perspectives, Chemosphere. 229 (2019) 188–199. https://doi.org/https://doi.org/10.1016/j.chemosphere.2019.04.193.

[64] F. Martins, S. Machado, T. Albergaria, C. Delerue-Matos, LCA applied to nano scale zero valent iron synthesis, Int. J. Life Cycle Assess. 22 (2017) 707–714. https://doi.org/10.1007/s11367-016-1258-7.

[65] S. Li, W. Yan, W. Zhang, Solvent-free production of nanoscale zero-valent iron (nZVI) with precision milling, Green Chem. 11 (2009) 1618–1626. https://doi.org/10.1039/B913056J.

[66] O. Hijazi, E. Abdelsalam, M. Samer, Y.A. Attia, B.M.A. Amer, M.A. Amer, M. Badr, H. Bernhardt, Life cycle assessment of the use of nanomaterials in biogas production from anaerobic digestion of manure, Renew. Energy. 148 (2020) 417–424. https://doi.org/https://doi.org/10.1016/j.renene.2019.10.048.